Soft x-ray absorption spectroscopy study of $(Ba_{0.5}Sr_{0.5})(Co_{0.8}Fe_{0.2})_{1-x}Nb_xO_{3-\delta}$ with different content of Nb (5%-20%)

Y.V. Egorova[1*], T. Scherb[2], G. Schumacher[2], H.J.M. Bouwmeester[3], E.O.Filatova[1]

[1] Institute of Physics, St-Petersburg State University, Ulyanovskaya Str. 3, Peterhof 198504, St. Petersburg, Russia

[2] Helmholtz-Zentrum Berlin für Materialien und Energie GmbH, Hahn-Meitner-Platz 1, D-14109 Berlin, Germany

[3] University of Twente, P.O. Box 217,7500 AE Enschede, The Netherlands

[*]Corresponding author: Yulia V Egorova
Email: Startjuli@gmail.com

Tobias Scherb
Email: tobias.scherb@helmholtz-berlin.de

Gerhard Schumacher
Email: schumacher@helmholtz-berlin.de

Henny J M Bouwmeester
Email: h.j.m.bouwmeester@tnw.utwente.nl

Elena O Filatova
Email: elenaofilatova@mail.ru

Abstract

The mixed electronic ionic conducting materials $(Ba_{0.5}Sr_{0.5})(Co_{0.8}Fe_{0.2})_{1-x}Nb_xO_{3-\delta}$ with partial Nb substitution (x: 0.05, 0.10, 0.15, 0.20) for B cations (Co/Fe), synthesized using a solid state reaction method, have been studied by near edge X-ray absorption fine structure (NEXAFS). Co $L_{2,3}$ - absorption spectra of $(Ba_{0.5}Sr_{0.5})(Co_{0.8}Fe_{0.2})_{1-x}Nb_xO_{3-\delta}$ (BSCFN) powders were analyzed with purpose to understand the influence of the Nb substitution on the atomic

electronic structure of BSCFN. The joint analysis of the Co $L_{2,3}$ - absorption spectra reveals the presence of mixed oxidation states Co^{2+}/Co^{3+} in all the studied BSCFN structures. It was established that the proportion of oxidation states Co^{2+}/Co^{3+} and the corresponding coordinations of Co atoms depend on the content of Nb. In the 10% Nb substituted BSCF sample Co atoms mostly occur in the Co^{2+} oxidation state and are preferentially characterized by octahedral coordination site. In all other structures Co atoms are rather characterized by Co^{2+}/Co^{3+} oxidation states and occupy both octahedrally and tetrahedrally coordinated sites.

Keywords

Solid oxide fuel cell, BSCF, microstructure, local bonding environment, NEXAFS

1. Introduction

Due to their good oxygen exchange performance, the highest oxygen permeation and mixed ionic and electronic conductivity, $Ba_{0.5}Sr_{0.5}Co_{0.8}Fe_{0.2}O_{3-\delta}$ (BSCF) oxides are potential candidates for cathode materials in solid oxide fuel cell (SOFC) applications [1, 2]. BSCF is an oxide mineral with perovskite structure (schematic formula of ABO_3). Ideal perovskites are characterized by cubic crystal structure. Cations in B position have octahedral coordination of oxygen anions and the voids between neighboring octahedra are filled with A- cations, coordinated by 12 oxygen ions. The crystal structure of perovskites depends on the ionic radii of oxygen anions and the cations. Goldschmidt introduced a tolerance factor (*t*), showing the deviation from the ideal cubic perovskite structure [3]:

$$t = \frac{r_A + r_O}{\sqrt{2(r_B + r_O)}},$$

where r_A, r_B, and r_o are the ionic radii of the A- and B- cations and of the oxygen anions, respectively. The cubic perovskite structure is preferred when $0.8 < t < 1$, while the formation of the hexagonal structure is preferred for $t > 1$. Analysis of BSCF structures shows that depending on the oxidation of the B-site cation, the tolerance factor of $Ba_{0.5}Sr_{0.5}Co_{0.8}Fe_{0.2}O_{3-\delta}$ varies within $0.97 < t < 1.07$ [4-6]. The mixed ionic and electronic BSCF conductors generally keep a significant concentration of oxygen vacancies (δ) [4,7,8]. A significant number of mobile oxygen vacancies makes BSCF excellent oxygen conductor and a good candidate for solid oxide fuel cell (SOFC) applications [8, 9] in the high temperature regime.

However, at intermediate temperatures (500°C-800°C) BSCF suffers from a slow decomposition of the cubic phase into a Co- and Ba enriched hexagonal phase and a cubic phase depleted in Co and Ba, resulting in a strong reduction of its performance [9, 10]. As follows from

[9-11], the instability of cubic BSCF at intermediate temperatures is predominantly connected with oxidation instability of the transition metal cations (mainly Co).

One way to solve the problem of phase stability of BSCF at intermediate temperatures is partial substitution of Nb for Co and Fe [5,12,13]. The stabilization effect of Nb for BSCF perovskite structure stems from the difference between interatomic distances in cubic and hexagonal perovskite structure. The distances between the Co/Fe ions and the oxygen ions (Co-O and Fe-O) in the hexagonal structure are shorter than in the cubic phase [13,14]. In accordance with the law of charge neutrality maintenance, the substitution of Nb^{5+} for Co atoms in BSCF system will lead to valence reduction of B-site elements and/or to decrease in the concentration of oxygen vacancies. The lowering of the B-site element oxidation state leads to increase of its ionic radius and thus to an increase in the bond length [13]. As a consequence of the substitution of Nb for (Co/Fe), B-site cations will preferentially take the cubic structure with longer distance between B cations.

It can be assumed that the substitution of Nb^{5+} for Co/Fe atoms in BSCF system, leading to valence reduction of B-site elements and/or to decrease in the concentration of oxygen vacancies, can be accompanied not only by a change in the interatomic distance Co-O and Fe-O but also by the alteration of the coordination number and local environment of the B- cation. Traditionally, BSCF compounds are investigated using the extended x-ray absorption fine structure (EXAFS) method. It is well known that EXAFS is due mostly to single scattering events of high-energy photoelectrons off the atomic cores by the neighboring atoms [15]. At the same time, when talking about identifying the distortion of the nearest environment of the central atom, NEXAFS studies seem appropriate. NEXAFS arises from excitations into unoccupied molecular orbitals and is dominated by multiple scattering of a low-energy photoelectron in the valence potential set up by the nearest neighbors. Often one can use a spectral "fingerprint" technique to identify the local bonding environment that defines the highest sensitivity of NEXAFS to distinguish chemical bonds and nearest polyhedral coordination sites. Thus NEXAFS provides the information about local (associated with a hole localization in the core shell) and partial (allowed for certain angular momentum symmetry) electronic density of states of the conduction band.

In this connection we attempted to study the $(Ba_{0.5}Sr_{0.5})(Co_{0.8}Fe_{0.2})_{1-x}Nb_xO_{3-\delta}$ perovskites with partial Nb substitution for Co/Fe depending on the Nb amount using NEXAFS.The goal of the current work is a study of the effect of Nb substitution of the B-site elements on the lowest unoccupied electronic states of the BSCF systems and as a consequence on the B coordination sites in the $(Ba_{0.5}Sr_{0.5})(Co_{0.8}Fe_{0.2})_{1-x}Nb_xO_{3-\delta}$ structure.

2. Experimental

All specimens of the mixed electronic ionic conducting materials $(Ba_{0.5}Sr_{0.5})(Co_{0.8}Fe_{0.2})_{1-x}Nb_xO_{3-\delta}$ with partial Nb substitution (x: 0.05, 0.10, 0.15, 0.20) for B-cations (Co/Fe) were synthesized nominally in the same way using a solid state reaction method. After synthesizing, the powder mixtures were dried, calcined in air at 950 °C and 1000 °C for 10 h at each temperature with intermediate milling in a mortar for 2h [12]. In the following, these materials will be denoted as BSCFN05, BSCFN10, BSCFN15, and BSCFN20, respectively. The NEXAFS measurements were performed at the RGL-station on the Russian-German beamline at the BESSY II synchrotron light source of the Helmholtz-Zentrum Berlin [16]. The spectra were measured at an incident angle of 45º in the vicinity of Co $L_{2,3}$- and Fe $L_{2,3}$ –absorption edges with energy resolution better than $E/\Delta E = 2000$. The spectra were obtained by monitoring the total electron yield (TEY) from the samples in the current mode. The energy scale was referenced to Au 4f 7/2 photoelectron peak (83.95 eV).

Angle dispersive X-ray diffraction (XRD) measurements were carried out with a *Bruker D8 Advance* diffractometer using Cu Kα radiation (wavelength $\lambda = 0.154$ nm).

3. Results and Discussion

The Co $L_{2,3}$- and Ba $M_{4,5}$- absorption spectra of Nb-substituted BSCF samples are shown in Fig. 1. The relative intensities of all the Co $L_{2,3}$- and Ba $M_{4,5}$- absorption spectra have been normalized to the continuum jump at the photon energy of 810 eV, after subtraction of a sloping background, which was extrapolated from the linear region below the Co $L_{2,3}$- and Ba $M_{4,5}$-absorption onset. All the studied absorption spectra consist of two groups of features A-B and A*-B*. The energy distances A-A* = 14.4 eV and B-B* = 14.7 eV agree well with the spin-orbit splitting of the Co 2p- and Ba 3d - levels in BSCF [17], respectively. The Co $2p_{1/2}$- and Ba $3d_{3/2}$-structures are marked by asterisks in Fig. 1. A joint analysis of all the studied spectra of BSCF samples does not reveal any visible differences in the shape and/or energy position of the features corresponding to Ba $M_{4,5}$-absorption spectrum (B and B*). On the other hand the shape of the spectra in the vicinity of the Co $L_{2,3}$-absorption edge depends on the Nb-content. The effect is more pronounced in the Co L_3- than in the L_2-absorption spectra. It is well known that the L_2 absorption spectra is misrepresented by an additional damping channel caused by the L_2L_3V- Coster-Kronig transition [18], which leads to the shorter life time of L_2- holes. We will, therefore, focus on the analysis of the evolution of the Co $2p_{3/2}$ -absorption spectra.

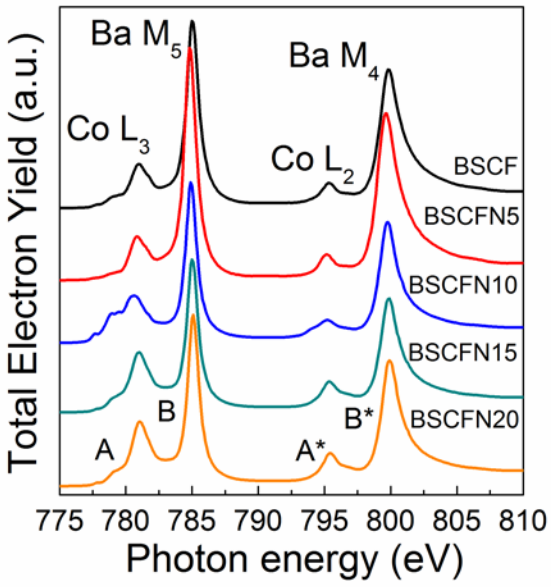

Fig.1. Co $L_{2,3}$- and Ba $M_{4,5}$- absorption spectra of BSCF systems with partial (5%, 10%, 15% and 20%) Nb substitution for B-site atoms. The details A and A* denote to Co $2p_{3/2}$ and Co $2p_{1/2}$, details B and B * denote to Ba $3d_{5/2}$- and Ba $3d_{3/2}$- levels, respectively.

The evolution of the shape of the Co$2p_{3/2}$- (Co L_3-) absorption spectra of Nb-substituted BSCF samples are shown in Fig. 2. Bearing in mind that the absorption spectra fine structure is very sensitive to the nature of the absorbing atoms, the chemical state and local coordination environment, it may expected to be a manifestation of different oxidation states of the Co atoms in CoL_3-absorption spectrum. The energy position of the metal L-edge shifts towards higher energies with increase of its oxidation state [9,19].

To understand the observed changes in Co L_3-absorption spectrum, the Co-L_3 absorption spectra of CoO- (oxidation state Co^{2+}) and Co_3O_4- (oxidation states Co^{3+}/Co^{2+}) structures were also analyzed (Fig. 2). The Co L_3-absorption spectrum of CoO was measured under the same experimental conditions as the absorption spectra of the Nb substituted BSCF samples whereas the Co L_3-absorption spectrum of Co_3O_4 was taken from [9].

In terms of the crystal field theory the energy levels of d-orbitals of the cation are split under the octahedrally (tetrahedrally) coordinated ligand-field into $t_{2g}(e_g)$ and $e_g(t_{2g})$ orbitals. As a result, both L_3 (and L_2) features are further split into doublet features. When comparing CoO and Co_3O_4 compounds, the balance between the crystal field splitting (Δ) (i.e., the energetic splitting between t_{2g}- and e_g- orbitals) and the exchange interaction (J) associated with Hund's rule should be considered [20, 21]. Depending on the values of Δ and J the electrons are redistributed differently between t_{2g}- and e_g- orbitals producing the different spin configurations.

CoO has a cubic crystal structure in which the Co^{2+}- ions are located in octahedral coordination (O_h) [20, 22, 23]. The ground state of Co^{2+} has an [Ar] $3d^7 4s^0$ configuration. According to the classical conception, the Co $2p_{3/2}$- absorption spectrum of CoO shows dipole allowed transitions of Co $2p_{3/2}$- electrons to unoccupied 3d states split by the octahedral crystal field created mainly by the O atoms [23,24]. The crystal field in CoO is relatively weak (the crystal field value (10Dq) of the ground state is ~ 1 eV [21]) that causes a high-spin configuration $t^5_{2g}e^2_g$ where the t_{2g}- orbitals are partly filled and therefore allow for low-energy d−d excitations. The ground term of the ground state of the Co^{2+} ion is ^4F, which is split on $^4T_{1g}(F)$, $^4T_{2g}$, $^4A_{2g}$ [21] features, and this explains the presence of the features **a-c** in the Co $L_{2,3}$- absorption spectrum of CoO (Fig. 2). Note that in a pure octahedral symmetry the crystal field value 10Dq is given by the energy difference between the $^4T_{2g}$ (4F) and the $^4A_{2g}$ (4F) states, and not by the energy difference between $^4T_{1g}$ (4F) and $^4T_{2g}$(4F), as $^4T_{1g}$(4F) is hybridized with the $^4T_{1g}$(4P) states [25,26].

In Co_3O_4 which has spinel-type structure cobalt ions exist in two different oxidation states, Co^{2+} and Co^{3+}. Co atoms can, therefore, occupy both octahedrally coordinated sites (16 sites for Co^{3+}) and tetrahedrally coordinated sites (8 sites for Co^{2+}) with the ratio 2:1 [27]. In Co_3O_4, the tetrahedral sites are occupied by Co^{2+} with high-spin state configuration $e^4_g t^3_{2g}$ (the ground term is $^4A_{2g}$) while the octahedral sites are occupied by Co^{3+} with low-spin state configuration $t^6_{2g}e^0_g$ (S=0, the ground term is $^1A_{1g}$). We stressed that in tetrahedral coordination there is the energetically reversed order of e_g and t_{2g} components compared with octahedral coordination. One can conclude that the Co $L_{2,3}$- absorption spectrum of Co_3O_4 corresponds to a mixture of Co^{3+} and Co^{2+} oxidation states (with ratio of 2:1). According to [23], the feature **d** of the Co $L_{2,3}$- absorption spectrum of Co_3O_4 reflects predominantly the Co^{2+}- states and feature **e** is formed mainly from the Co^{3+}- states.

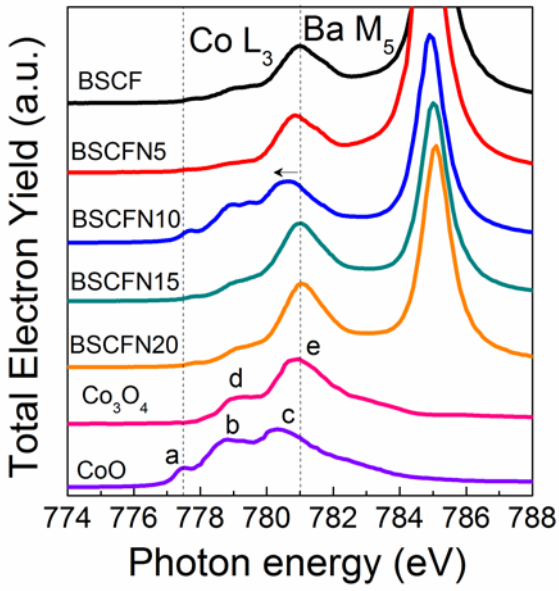

Fig.2. Co L_3- absorption spectra of Nb substituted BSCF systems, compared with Co L_3-absorption spectra of CoO and Co_3O_4 systems. The absorption spectrum of Co_3O_4 is taken from [9]. The denotations **a**-**d** used to describe features of Co L_3- absorption spectra are explained in the text.

The joint analysis of the absorption spectra of all the studied BSCF structures in Fig. 2 reveals that the shape of the CoL_3-absorption spectrum depends on the Nb-substitution in B position. The most noticeable changes are traced in the CoL_3-absorption spectrum of BSCFN10: i) the spectrum is shifted towards lower energies by about 0.5 eV with respect to the spectra of all the other samples; ii) more higher intensity of a shoulder denoted by (**a**) in Fig. 2, which is hardly visible in the spectra of the other specimens. In the number of features and their energy positions the $CoL_{2,3}$- absorption spectrum of BSCF samples with 10 % Nb substitution Co atoms correlates well with the CoL_3-absorption spectrum of CoO where the Co^{2+} ions are located in octahedral coordination. The spectra of all the other BSCF samples are more similar to the CoL_3-absorption spectrum of Co_3O_4 with small part of CoL_3-absorption spectrum of CoO (appearance of the weak feature **a**).

It is plausible to assume that the Co oxidation state in Nb substituted BSCF depends on the Nb content. The change of Co oxidation state is greater in BSCFN10 than in all the other samples. The joint analysis of the CoL_3-absorption spectra of all the studied BSCF structures reveals that in the BSCF samples with 5, 15, 20 % Nb substitution, Co atoms occupy sites with mixed oxidation states Co^{2+}/Co^{3+} and as a consequence, octahedrally and tetrahedrally

coordinated sites. Co atoms in BSCFN10 are predominantly characterized by a valence of 2^+ and occupy predominantly octahedrally coordinated sites.

The possibility of phase transformation from Co_3O_4 to CoO was traced in different NEXAFS [28] and XPS [29] studies. In particular, according to [29], the main peaks of Co $2p_{3/2}$ and Co $2p_{1/2}$ in CoO upshift by 0.8 eV in contrast to Co_3O_4. This shift is due to the change of coordination environment of Co ions from Co_3O_4 to CoO. This observation is an additional evidence of our conjecture that Co atoms in BSCF sample with 10% Nb substitution are predominantly characterized by a valence of 2^+.

In an orderly sequence of BSCF with partial Nb substitution of model BSCF, BSCFN05, BSCFN10, BSCFN15 and BSCFN20 the branching ratio I_2/I_3 (where I_2 and I_3 are the integral intensities of the L_2 and L_3 peaks, respectively) for Co $L_{2,3}$-absorption edges is equal to 0.40, 0.41, 0.27, 0.43 and 0.43, respectively. The uncertainty is about 0.05, and is specified by the accuracy determining the values of the intensities and also by the accuracy of elicitation of the Ba-$M_{4,5}$-absorption spectra features and, as a consequence, by accuracy of background subtraction for Co $L_{2,3}$-absorption spectra features. It is evident that in the considered sequence the ratio L_2/L_3 is near 0.4 and decreases to value ~0.3 for BSCF with 10% Nb substitution.

Within the independent particle approximation the so-called branching ratio between the L_2 and L_3 edges is determined by the occupation numbers of the corresponding core states and gives 1:2 [30]. However, according to [30, 31], a deviation of the branching ratio L_2/L_3 from its statistical value in 3d elements is traced. A similar problem of the ratio between the L_β- and L_α-line intensities of 3d transition metal oxides was studied in x-ray emission spectra [18]. In [18] the existence of the integrated-intensity ratio of L_β- and L_α- lines on the atomic magnetic moment has been established.

The deviation of the branching ratio L_2/L_3 from its statistical value is due to the interaction of the exited electron with its core hole (due to the localization of the core wave function), which is very strong in the case of 3d- elements and cannot be ignored. It is important that according to [31], exchange term does not depend on the screening but is related to a coherent mixing between the excitations from $2p_{1/2}$- and $2p_{3/2}$- core levels in 3d- elements. As follows from the [31] this effect is proportional to the size of the spin-orbit splitting and becomes smaller for later transition metals. For titanium oxides, as an example, the ratio L_2/L_3 is close to 1:1. With respect to late transition metal compounds, according to [32] the number of unpaired 3d- electrons reduces in the creation of the core hole, i.e., they do not represent the ground-state spin state for these compounds (but conserves for early transition metal compounds).The dipole selection rules make the spectra strongly depending on the symmetry of the initial state of the Co ions. According to [33,34,35], in a high-spin state the exchange coupling between the core-hole

and 3*d* electrons tends to reduce noticeably the branching ratio from ½, while in the case when the Co ions mainly have the local low-spin state character the branching ratio differs from ½ only slightly. Analysis of the values obtained for studied BSCF with partial Nb substitution allows to conclude that the ratio L_2/L_3 is 0.4 in all the samples apart from BSCFN10 indicating that the Co ions in these samples mainly have the local low-spin state character (Co^{3+} state). In the sample BSCFN10, Co ions mainly have the local high-spin state character (Co^{2+} state). The observed change in the branching ratio L_2/L_3 is an additional proof related to change in the oxidation state of Co atom in BSCFN10 sample.

It should be mentioned that Fe $L_{2,3}$ -absorption spectra of the same BSCF structure were also studied. However, the joint analysis of Fe $L_{2,3}$-absorption spectra measured for BSCF structure with different Nb substitution did not reveal noticeable changes in the spectra that agree well with concepts of the role of the Fe atom in the BSCF structure: in the perovskite oxide BSCF the Fe atoms in contrast to the Co atoms are more resistant to changes in the oxidation state [9]. For this reason the Fe $L_{2,3}$ -absorption spectra are not discussed in the current paper.

As was mentioned above, the lowering of the element oxidation state leads to increase of the ionic radius. The ionic radii of Co^{3+}- and Co^{2+}- oxidation states are 0.0545 nm (low spin) and 0.0745 nm (high spin)[36]. According to the Goldschmidt tolerance factor [3], the increase of the ionic radius B caused by lowering the oxidation state of B cation should stabilize the cubic phase of BSCF structures. Thus it is more reasonable to expect phase stabilization in the BSCF sample with 10% Nb substitution, for which the change in the oxidation state from Co^{2+}/Co^{3+} aside to Co^{2+} was established.

The exceptional behavior of BSCF might be understood regarding the results from XRD measurements, see Fig. 3.

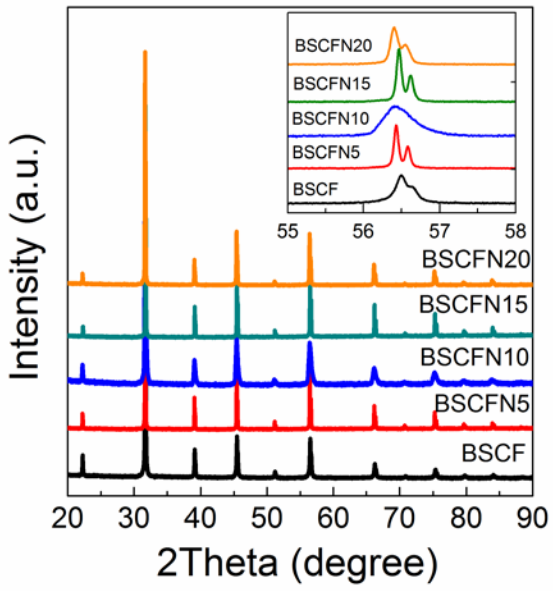

Fig.3. XRD patterns of Nb substituted BSCF systems. The (211) reflection is shown in the inset.

All reflections can be indexed by the cubic perovskite structure with Pm-3m space group. The powder containing 10 % Nb on B-site, BSCFN10 reveals qualitatively different diffraction patterns than the other three powders BSCFN05, BSCFN15 and BSCFN20. While the reflections of the latter three powders reveal sharp reflections with peaks split into $K_{\alpha 1}$ and $K_{\alpha 2}$ sub-peaks, this kind of splitting is not observed for BSCFN10. Instead, BSCFN10 reveals broad reflections which point to either crystallite sizes on the nm scale, i.e., to crystallites with mean size below 100 nm, or to a distribution in chemical composition causing a variety of lattice parameters and thus broadening of lattice reflections. The origin of the peak broadening in BSCFN10 is not quite clear and the peak broadening observed for BSCFN10 is in disagreement to the results from XRD measurements of Fang et al. [12] which yielded XRD pattern with small peak widths for all four powders, BSCFN05, BSCFN10, BSCFN15 and BSCFN20. Additional treatment of BSCFN10 at 1000°C for 11 h caused slight narrowing of the diffraction peaks indicating increase in grain size, decrease of stresses or homogenization of chemical fluctuations. The structure remained, however, very different from those of the other powders.

Further evidence for the exceptional structure of BSCFN10 is given by neutron diffraction measurements which revealed orthorhombic crystal structure with Pnma space group [37] in contradiction to the XRD results of Fang et al. [12]. Hence, further research is required to solve the puzzling structure of BSCFN10.

4. Conclusions

The mixed electronic ionic perovskite oxide BSCF with partial Nb substitution (5% - 20%) for Fe and Co on the B-site has been studied by NEXAFS technique. Joint analysis of the Co L_3-absorption spectra of Nb substituted BSCFN, CoO- and Co_3O_4- structures testified that only in BSCFN10 samples Co occurs in the oxidation state close to Co^{2+}. In all other structures Co atoms are rather characterized by mixed oxidation states Co^{2+}/Co^{3+}.

Acknowledgment

The authors acknowledge financial support from the German-Russian Interdisciplinary Science Center (G-RISC, DAAD, projects P-2013a-8, P-2014a-11). We thank HZB for the allocation of synchrotron radiation beamtime. Support from Helmholtz-Association through the Helmholtz-Alliance MEM-BRAIN is also gratefully acknowledged.

References

[1] Z.P. Shao, S.M. Haile, A high-performance cathode for the next generation of solid-oxide fuel cells, Nature 431 (2004) 170–173.

[2] W. Zhou, R. Ran, Z. Shao, Progress in understanding and development of $Ba_{0.5}Sr_{0.5}Co_{0.8}Fe_{0.2}O_{3-\delta}$-based cathodes for intermediate-temperature solid-oxide fuel cells: A review, J. Power Sources 192 (2009) 231–246.

[3] V.M. Goldschmidt, Die Gesetze der Krystallochemie Naturwissenschaften 14 (1926) 477-485. doi: 10.1007/BF01507527.

[4] S. McIntosh, J.F. Vente, W.G. Haije, et al., Structure and oxygen stoichiometry of $SrCo_{0.8}Fe_{0.2}O_{3-\delta}$ and $Ba_{0.5}Sr_{0.5}Co_{0.8}Fe_{0.2}O_{3-\delta}$, Solid State Ionics 177 (2006) 1737–1742.

[5] Y. Li, H. Zhao, N. Xu, et al., Systematic investigation on structure stability and oxygen permeability of Sr-doped $BaCo_{0.7}Fe_{0.2}Nb_{0.1}O_{3-\delta}$ ceramic membranes, Journal of Membrane Science 362 (2010) 460–470. doi: 10.1016/j.memsci.2010.06.065.

[6] B. Liu, Y. Zhang, L. Tang, X-ray photoelectron spectroscopic studies of $Ba_{0.5}Sr_{0.5}Co_{0.8}Fe_{0.2}O_{3-\delta}$ cathode for solid oxide fuel cells, Int. J. Hydrogen Energy 34(2009) 435-439.

[7] S. McIntosh, J.F. Vente, W.G. Haije, et al., Oxygen stoichiometry and chemical expansion of Ba0.5Sr0.5Co0.8Fe0.2O3-δ measured by in situ neutron diffraction, J. Chem. Mater. 18 (2006) 2187–2193. doi: 10.1021/cm052763x.

[8] M.M. Kuklja, Y.A. Mastrikov, B. Jansang, E.A. Kotomin, The intrinsic defects, disordering, and structural stability of $Ba_xSr_{1-x}Co_yFe_{1-y}O_{3-\delta}$ perovskite solid solutions, J. Phys. Chem. C 116(35) (2012) 18605−18611. doi: 10.1021/jp304055s.

[9] M. Arnold, Q. Xu, F.D. Tichelaar, A. Feldhoff, Local charge disproportion in a high-performance perovskite, J. Chem. Mater. 21(4) (2009) 635–640. doi: 10.1021/cm802779f.

[10] K. Efimov, Q. Xu, A. Feldhoff, Transmission electron microscopy study of $Ba_{0.5}Sr_{0.5}Co_{0.8}Fe_{0.2}O_{3-\delta}$ perovskite decomposition at intermediate temperatures. J Chem Mater. 22(21) (2010) 5866–5875. doi: 10.1021/cm101745v.

[11] F. Liang, H. Jiang, H. Luo, et al., Phase stability and permeation behavior of a dead-end $Ba_{0.5}Sr_{0.5}Co_{0.8}Fe_{0.2}O_{3-\delta}$ tube membrane in high-purity oxygen production, J. Chem. Mater. 23(21) (2011) 4765–4772. doi: 10.1021/cm2018086.

[12] S.M. Fang, C.-Y. Yoo, H.J.M. Bouwmeester, Performance and stability of niobium-substituted $Ba_{0.5}Sr_{0.5}Co_{0.8}Fe_{0.2}O_{3-\delta}$ membranes, J Solid State Ionics 195 (2011) 1–6.

[13] Y. Cheng, H. Zhao, D. Teng, et al., Investigation of Ba fully occupied A-site $BaCo_{0.7}Fe_{0.3-x}Nb_xO_{3-\delta}$ perovskite stabilized by low concentration of Nb for oxygen permeation membrane, Journal of Membrane Science 322 (2008) 484–490.

[14] P. Müller, M. Meffert, H. Störmer, D. Gerthsen, Fast mapping of the cobalt-valence state in $Ba_{0.5}Sr_{0.5}Co_{0.8}Fe_{0.2}O_{3-\delta}$ by electron energy loss spectroscopy, J. Microsc. Microanal. 19 (2013) 1595–1605.

[15] J. Stöhr, NEXAFS Spectroscopy, Springer-Verlag, Berlin, 1992.

[16] S.I. Fedoseenko, I.E. Iossifov, S.A. Gorovikov, J.-H. Schmidt, R. Follath, S.L. Molodtsov, V.K. Adamchuk and G. Kaindl, Development and present status of the Russian–German soft X-ray beamline at BESSY II, Nuclear Instruments and Methods in Physics Research A 470 (2001) 84-88. doi:10.1016/S0168-9002(01)01032-4.

[17] J.-I.I. Jung, D.D. Edwards, X-ray photoelectron (XPS) and Diffuse Reflectance Infra Fourier Transformation (DRIFT) study of $Ba_{0.5}Sr_{0.5}Co_xFe_{1-x}O_{3-\delta}$ (BSCF: x=0–0.8) ceramics, Journal of Solid State Chemistry 184 (2011) 2238–2243. doi: 10.1016/j.jssc.2011.06.016.

[18] V.I. Grebennikov, V.R. Galakhov, L.D. Finkel'shtein, et al., Effect of atomic magnetic moments on the relative intensity of the L_β and L_α components in X-ray emission spectra of 3d transition metal oxides, Phisics of the Solid State V 45(6) (2003) 1048-1055. doi: 10.1134/1.1583787.

[19] J. Taftø and O.K. Krivanek, Site-specific valence determination by Electron Energy-Loss Spectroscopy, J. Phys. Rev. Lett. 48 (1982) 560.

[20] M. Magnuson, S.M. Butorin, J.-H. Guo, J. Nordgren, Electronic structure investigation of CoO by means of soft x-ray scattering, J. Phys. Rev. B 65 (2002) 205106.

[21] M.M. Schooneveld, R. Kurian, A. Juhin, et al., Electronic structure of CoO nanocrystals and a single crystal probed by Resonant X-ray Emission Spectroscopy, J. Phys. Chem. C 116(29) (2012) 15218−15230. doi: 10.1021/jp302847h.

[22] A.F. Wells, Structural Inorganic Chemistry, Clarendon Press, London, 1950.

[23] F. Morales, F.M. De Groot, P. Glatzel, et al., In situ X-ray absorption of Co/Mn/TiO2 catalysts for fischer-tropsch synthesis, J. Phys. Chem. B 108(41) (2004) 16201-16207. doi: 10.1021/jp0403846.

[24] U. Fano, J.W. Cooper, Spectral distribution of atomic oscillator strengths, Rev. Mod. Phys. 40 (1968) 441.

[25] Y. Tanabe, S. Sugano, On the Absorption spectra of complex ions. I, J Physical Society of Japan, 9 (1954) 753-766. doi: http://dx.doi.org/10.1143/JPSJ.9.753.

[26] A.B.P. Lever, Inorganic Electronic Spectroscopy (2nd ed), Elsevier, Amsterdam, The Netherlands, 1984.

[27] M.-Y. Li, P. Shen, On the nucleation and paracrystal interspacing of Zr-doped $CO_{3-delta}O_4$, J. Materials Science and Engineering B 111(1) (2004) 82–89. doi: 10.1016/j.mseb.2004.04.007.

[28] D. Bazin, I. Kovács, L. Guczi, et al., Genesis of Co/SiO_2 catalysts: XAS study at the Cobalt $L_{III,II}$ absorption edges, Journal of Catalysis 189 (2000) 456–462. doi: 10.1006/jcat.1999.2654.

[29] S. Zhang, J.-j. Shan, Y. Zhu, et al., WGS catalysis and In Situ studies of CoO_{1-x}, $PtCo_n/Co_3O_4$, and $Pt_mCo_{m'}/CoO_{1-x}$ nanorod catalysts, J. American Chemical Society 135 (2013) 8283−8293. doi: 10.1021/ja401967y.

[30] B.T. Thole, G. Van der Laan, Branching ratio in x-ray absorption spectroscopy, J. Phys. Rev. B 38(3) (1988) 3158.

[31] R. Laskowski, P. Blaha, Understanding the $L_{2,3}$ x-ray absorption spectra of early 3d transition elements, J. Phys. Rev. B 82 (2010) 205104.

[32] C. Suzuki, J. Kawai, H. Adachi, T. Mukoyama, Electronic structures of 3d transition metal (Ti–Cu) oxides probed by a core hole, J. Chemical Physics 247(3) (1999) 453–470. doi:10.1016/S0301-0104(99)00212-8.

[33] T. Mizokawa, L.H. Tjeng, P.G. Steeneken, et al., Photoemission and x-ray-absorption study of misfit-layered (Bi,Pb)-Sr-Co-O compounds: Electronic structure of a hole-doped Co-O triangular lattice, J. Phys. Rev. B 64 (2001) 115104.

[34] F.M. De Groot, J.C. Fuggle, B.T. Thole, G.A. Sawatzky 2p x-ray absorption of 3d transition-metal compounds: An atomic multiplet description including the crystal field. J Phys Rev B 42 (1990) 5459–5468.

[35] J.L. Chen, Y.S. Liu, C.-J. Liu, et al., X-ray absorption spectroscopy studies of $Ca_{2.9}Ln_{0.1}Co_4O_{9+\delta}$ (Ln = Ca, Dy, Ho, Er and Lu), Journal of Alloys and Compounds 529 (2012) 8-11.

[36] H.S.C. O'Neill, A. Navrotsky, Simple spinels; crystallographic parameters, cation radii, lattice energies, and cation distribution, J American Mineralogist 68 (1983) 181-194.

[37] C.Y. Yoo, J. Kohnke, G. Schumacher, H.J.M. Bouwmeeseter, Unpublished results.